INTERNATIONAL JOURNAL OF
ENERGY AND ENVIRONMENT

Volume 7, Issue 1, 2016 pp.61-76
Journal homepage: www.IJEE.IEEFoundation.org

Exergy analysis for combined regenerative Brayton and inverse Brayton cycles with regeneration after the inverse cycle

Zelong Zhang[1,2,3], Lingen Chen[1,2,3], Yanlin Ge[1,2,3], Fengrui Sun[1,2,3]

[1] Institute of Thermal Science and Power Engineering, Naval University of Engineering, Wuhan 430033.
[2] Military Key Laboratory for Naval Ship Power Engineering, Naval University of Engineering, Wuhan 430033.
[3] College of Power Engineering, Naval University of Engineering, Wuhan 430033, China.

Abstract
Exergy analysis and optimization is carried out for combined regenerative Brayton and inverse Brayton cycles with regenerator after the inverse cycle. The analytical formulae of exergy efficiency of the combined cycle and exergy losses of each component are derived. The largest exergy loss location is determined. It is shown that exergy efficiency increases with the increase in the effectiveness of regenerator in the critical range of the compressor pressure ratio of the bottom cycle. Furthermore, the exergy loss of combustion chamber is the largest in the combined cycle.

Keywords: Regenerative Brayton cycle; Inverse Brayton cycle; Combined cycle; Exergy analysis; Exergy efficiency; Exergy loss; Optimization.

1. Introduction

As the industrial revolution happened after the second half of the twentieth century, the increasing utilization of the new technological products in our daily life caused more consumption of energy. In this situation, people want to construct new power and energy plants which could gain more efficiency from energy sector.

For the improvements of the energy systems, there are two basic methods including energy analysis and exergy analysis. The exergy analysis method [1-14] provides a more accurate measurement of the system efficiency than the energy analysis and determines the exergy loss location of the energy systems.

Steam and gas turbine combined cycles are considered as the most effective power plants whose application is becoming more and more common in mid and large scale power production [15]. The thermal efficiency of these cycle types exceeded 55 percent several years ago and is now at approximately 60 percent. In order to increase the power output, Braysson cycle (a hybrid gas turbine cycle) was proposed based on a conventional Brayton cycle for the high temperature heat addition process and an Ericsson cycle for the low temperature heat rejection process, and the energy analysis of the Braysson cycle was performed by Frost et al. [16] in 1997. Furthermore, the exergy analysis of the Braysson cycle was carried out by Zheng et al. [17] in 2001. Fujii et al. [18] studied a combined-cycle which composed with a top cycle (Brayton cycle) and a bottom cycle consisting of an expander followed by an inter-cooled compressor in 2001. It was found that when fixed the bottom cycle pressure ratio to

0.25 bar could avoid a rapid increase in gas flow axial velocity effectively. The use of two parallel inverse Brayton cycles instead of one was proposed in order to reduce the size of the overall power plant. Bianchi et al. [19] studied a combined-cycle consisting of a top cycle (Brayton cycle) and a bottom cycle (an inverse Brayton cycle in which air is compressed to atmospheric pressure) in 2002. Agnew et al. [20] proposed combined Brayton and inverse Brayton cycles in 2003, and performed the energy analysis of the combined cycle. It was found that the optimal expansion pressure of the inverse Brayton cycle is 0.5 bar for the optimum performance. Zhang et al. [21] performed the exergy analysis and optimization of the combined Brayton and inverse Brayton cycles in 2007. They found that exergy loss of combustion is the biggest in the cycle and followed by heat exchanger. Based on the combined Brayton and inverse Brayton cycles, Alabdoadaim et al. [22] proposed its developed configurations including regenerative cycle and reheat cycle, and they found that the use of regenerative Brayton cycle as top cycle can obtain higher thermal efficiency than the base cycle but with smaller work output based on energy analysis. Zhang et al. [23] performed the exergy analysis and optimization of the combined regenerative Brayton and inverse Brayton cycles with regeneration before the inverse cycle. Compared with combined regenerative Brayton and inverse Brayton cycles with regeneration before the inverse cycle proposed in Ref. [22], Zhang et al. [24] proposed a new combined cycle configuration with regeneration after the inverse cycle in order to keep work output of the combined cycle and studied the performance of the new combined cycle based on energy analysis.

In this paper, the exergy analysis for combined regenerative Brayton and inverse Brayton cycles with regeneration after the inverse cycle [24] will be performed. The purposes of the study are to determine the largest exergy loss location and optimize the exergy efficiency of the combined cycle by adjusting pressure ratio of the compressor of the regenerative Brayton cycle.

2. Cycle model

The proposed system in Ref. [24] is shown in Figure 1. It is constructed from a top regenerative Brayton cycle and a bottom inverse Brayton cycle. The top cycle is used as a gas generator to power the bottom cycles. The purpose of the turbine in the top cycle is solely to power the compressor. The power output of the combined cycle is totally produced by the bottom cycle. The energy performance analysis of the system was studied in Ref. [24]. Figure 2 shows T-s diagrams of the system. Process 1-2 is an irreversible adiabatic compression process in the compressor 1. Process 2-3 is an absorbed heat process in the regenerator. Process 3-4 is an absorbed heat process in the chamber. Process 4-5 is an irreversible adiabatic expansion process in the turbine 1. Process 5-6 is an irreversible adiabatic expansion process in the turbine 2. Process 6-7 is an evolved heat process in the regenerator. Process 7-8 is an evolved heat process in the heat exchanger. Process 8-9 is an irreversible adiabatic compression process in the compressor 2.

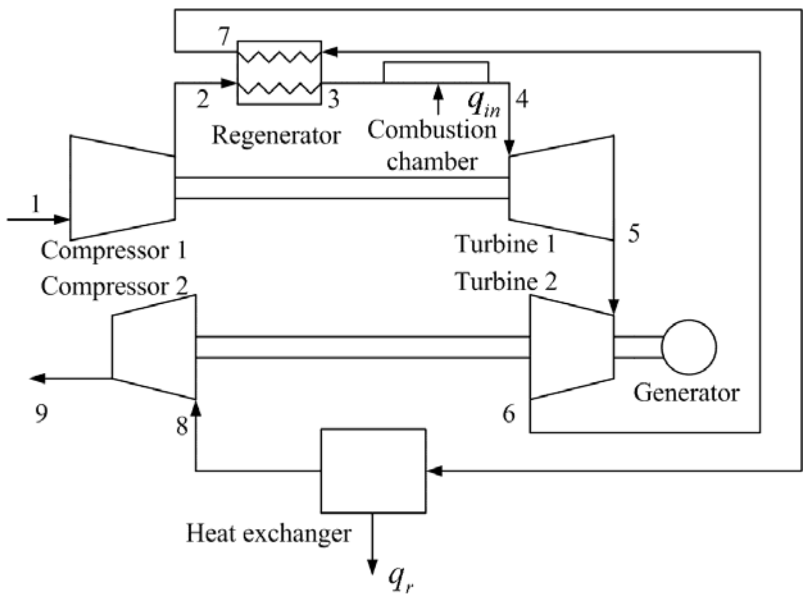

Figure 1. System layout of the combined cycle

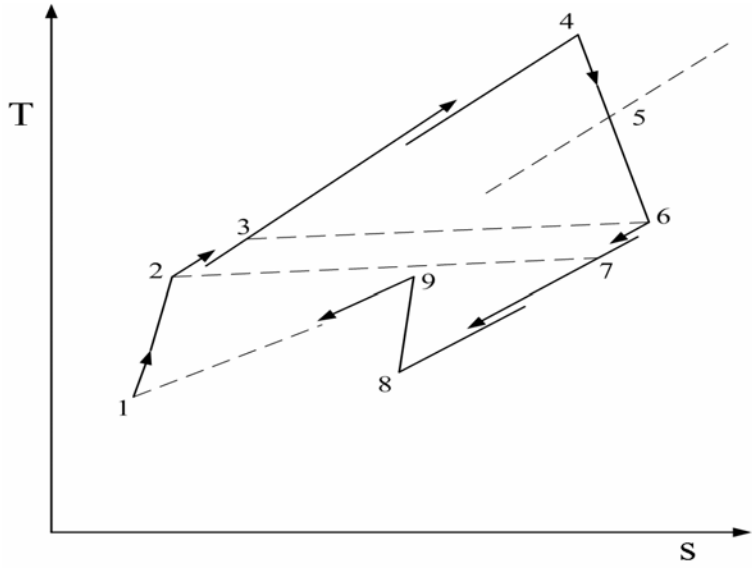

Figure 2. T-s diagram for the combined cycle

3. Exergy analysis and optimization

The following assumptions are made for simplicity and manipulating analytical expressions: The working fluid has constant specific heat ratio k ($k = c_P / c_V = 1.4$). The mass flow rate $\dot{m}$ is fixed as 1 kg/s.

For the system operating in a steady state, the general exergy balance equation is given in Refs. [3-9]. After making an exergy balance equation, the expression of the exergy balance equation can be obtained for each component, respectively.

For the compressor 1, the following expression can be obtained:

$$w_{c1} = (e_2 - e_1) + e_{D.c1} \tag{1}$$

where $w_{c1} = c_p T_1 \psi_{c1} / \eta_{c1}$ is specific work consumed of the compressor 1, c_p is constant-pressure specific heat, T is temperature, $\psi_{c1} = \varphi_{c1}{}^m - 1$, $m = (k-1)/k$, $\varphi_{c1} = P_2 / P_1$ is pressure ratio of compressor 1, P is pressure, e is exergy, η_{c1} is the efficiency of the compressor 1, and $e_{D.c1} = c_p T_1 \left[\text{In}(1 + \psi_{c1}/\eta_{c1}) - m\text{In}\varphi_{c1} \right]$ is exergy loss of the compressor 1.

For the turbine 1, the following expression can be obtained:

$$w_{t1} + (e_5 - e_4) + e_{D.t1} = 0 \tag{2}$$

where $w_{t1} = c_p T_1 \tau_1 \psi_{t1} \eta_{t1}$ is specific work output of the turbine 1, $\psi_{t1} = 1 - 1/\varphi_{t1}{}^m$, $\varphi_{t1} = P_4 / P_5$ is pressure ratio of turbine 1, $e_{D.t1} = c_P T_1 \left[\text{In}(1 - \eta_{t1}\psi_{t1}) - m\text{In}(1/\varphi_{t1}) \right]$ is exergy loss of turbine 1, and η_{t1} is efficiency of the turbine 1.

For the turbine 2, the following expression can be obtained:

$$w_{t2} + (e_6 - e_5) + e_{D.t2} = 0 \tag{3}$$

where $w_{t2} = c_p T_1 \eta_{t2} \psi_{t2} (\tau_1 - \psi_{c1}/\eta_{c1})$ is specific work output of the turbine 2, $\psi_{t2} = 1 - 1/\varphi_{t2}{}^m$, $\varphi_{t2} = P_5 / P_6$ is pressure ratio of the turbine 2, $\tau_1 = T_4 / T_1$ is temperature ratio, η_{t2} is efficiency of the turbine 2, and $e_{D.t2} = C_p T_1 \left[\ln(1 - \eta_{t2}\psi_{t2}) - m\ln(1/\varphi_{t2}) \right]$ is exergy loss of the turbine 2.

For the combustion chamber, the following expression can be obtained:

$$e_f = (e_4 - e_3) + e_{D.f} \tag{4}$$

ISSN 2076-2895 (Print), ISSN 2076-2909 (Online)

where: $e_f = q_{in}/\eta_b$ is exergy of fuel, η_b is efficiency of combustion chamber, $q_{in} = c_p T_1 \left[\tau_1 - E_R \tau_1 (1-\eta_{t1}\psi_{t1})(1-\eta_{t2}\psi_{t2}) - (1-E_R)(\psi_{c1}+\eta_{c1})/\eta_{c1}\right]$ is absorbed heat of the system, h is enthalpy, $e_{D.f} = c_p T_1 \ln\left[\frac{\tau_1\eta_{c1}}{(1-E_R)(\psi_{c1}+\eta_{c1}) + E_R\tau_1(1-\eta_{t1}\psi_{t1})(1-\eta_{t2}\psi_{t2})\eta_{c1}D_2^m}\right] + c_p T_1 (1/\eta_b - 1)\left[\tau_1 - (1-E_R)(\psi_{c1}+\eta_{c1})/\eta_{c1} + E_R\tau_1(1-\eta_{t1}\psi_{t1})(1-\eta_{t2}\psi_{t2})\right]$ is exergy loss of the combustion chamber, E_R is effectiveness of the regenerator, $D_2 = 1-\Delta P_{3-4}/P_3$ is pressure recovery coefficient, and $\Delta P_{3-4} = P_3 - P_4$.

For the regenerator, the following expression can be obtained:

$$e_{D.re} + (e_3 - e_2) + (e_7 - e_6) = 0 \tag{5}$$

where $e_{D.re} = c_p T_1 \ln\left[E_R \frac{\tau_1(1-\eta_{t1}\psi_{t1})(1-\eta_{t2}\psi_{t2})\eta_{c1}}{\psi_{c1}+\eta_{c1}} + 1 - E_R\right] \times \left[E_R \frac{\psi_{c1}+\eta_{c1}}{\tau_1(1-\eta_{t1}\psi_{t1})(1-\eta_{t2}\psi_{t2})\eta_{c1}} + 1 - E_R\right] - c_p T_1 m \ln D_1 D_3$ is exergy loss of the regenerator, $D_1 = 1-\Delta P_{2-3}/P_2$ ($\Delta P_{2-3} = P_2 - P_3$) and $D_3 = 1-\Delta P_{6-7}/P_6$ ($\Delta P_{6-7} = P_6 - P_7$) are pressure recovery coefficients.

For the heat exchanger, the following expression can be obtained:

$$(e_8 - e_7) + e_{HE} = 0 \tag{6}$$

where: $e_{HE} = c_p T_1 \ln\left[(1-\varepsilon) + \frac{\varepsilon}{E_R(\psi_{c1}+\eta_{c1})/\eta_{c1} + \tau_1(1-E_R)(1-\eta_{t1}\psi_{t1})(1-\eta_{t2}\psi_{t2})}\right] - c_p T_1 \left\{\ln D_4^m + \varepsilon - \varepsilon\left[E_R(\psi_{c1}+\eta_{c1})/\eta_{c1} + \tau_1(1-E_R)(1-\eta_{t1}\psi_{t1})(1-\eta_{t2}\psi_{t2})\right]\right\}$ is exergy loss of the heat exchanger, ε is effectiveness of the heat exchanger, and $D_4 = 1-\Delta P_{7-8}/P_7$ ($\Delta P_{7-8} = P_7 - P_8$) is pressure-recovery coefficient.

For the compressor 2, the following expression can be obtained:

$$w_{c2} = (e_9 - e_8) + e_{D.c2} \tag{7}$$

where $w_{c2} = c_p T_1\{[E_R(1+\psi_{c1}/\eta_{c1}) + \tau_1(1-E_R)(1-\eta_{t1}\psi_{t1})(1-\eta_{t2}\psi_{t2})](1-\varepsilon)+\varepsilon\}\psi_{c2}/\eta_{c2}$ is specific work consumed of the compressor 2, η_{c2} is efficiency of the compressor 2, $e_{D.c2} = c_p T_1\left[\ln(1+\psi_{c2}/\eta_{c2}) - m\ln\varphi_{c2}\right]$ is exergy loss of the compressor 2, $\psi_{c2} = \varphi_{c2}{}^m - 1$ and $\varphi_{c2} = P_9/P_8$ is pressure ratio of the compressor 2.

For the exhaust gas of the inverse Brayton cycle, the following expression can be obtained:

$$e_9 - e_1 = e_{ex} \tag{8}$$

where $e_{ex} = c_p T_1\{(1+\psi_{c2}/\eta_{c2})\{[E_R(1+\psi_{c1}/\eta_{c1}) + \tau_1(1-E_R)(1-\eta_{t1}\psi_{t1})(1-\eta_{t2}\psi_{t2})](1-\varepsilon)+\varepsilon\} - [m\ln(1/D_0)-1]\}c_p T_1 \ln\{(1+\psi_{c2}/\eta_{c2})/\{[E_R(1+\psi_{c1}/\eta_{c1}) + \tau_1(1-E_R)(1-\eta_{t1}\psi_{t1})(1-\eta_{t2}\psi_{t2})](1-\varepsilon)+\varepsilon\}\}$ is exergy loss of the exhaust gas, and $D_0 = P_1/P_9$.

For the turbine 1 is solely used to power the compressor 1 ($w_{c1} = w_{t1}$), one can derive the following expression:

$$\varphi_{t1} = \left[\eta_{c1}\eta_{t1}\tau_1 / (\eta_{c1}\eta_{t1}\tau_1 - \varphi_{c1}{}^m + 1)\right]^{\frac{1}{m}} \tag{9}$$

For the total pressure ratios of expansion and compression are equal ($\varphi_{t2} = D\varphi_{c1}\varphi_{c2}/\varphi_{t1}$), one can derive the following expression:

$$\psi_{t2} = 1 - \frac{\eta_{c1}\eta_{t1}\tau_1}{D^m(\psi_{c1}+1)(\eta_{c1}\eta_{t1}\tau_1 - \psi_{c1})\varphi_{c2}^m} \tag{10}$$

where $D = D_0 D_1 D_2 D_3 D_4$ is total pressure-recovery coefficient.

The specific work and the exergy efficiency of the combined cycle are defined as:

$$\begin{aligned} w = w_{t2} - w_{c2} = c_p T_1\{\eta_{t2}(1 - a/\varphi_{c2}^m)b - \\ [E_R c(1-\varepsilon) - b\eta_{t2}(1-E_R)(1-\eta_{t2}+\eta_{t2}\, a/\varphi_{c2}^m)(1-\varepsilon)+\varepsilon](\frac{\varphi_{c2}^m - 1}{\eta_{c2}})\} \end{aligned} \tag{11}$$

$$\eta_E = w/e_f = \frac{\begin{array}{c}\eta_{t2}(1-a/\varphi_{c2}^m)b - [E_R c(1-\varepsilon) - b\eta_{t2}(1-E_R) \\ \times(1-\eta_{t2}+\eta_{t2}\, a/\varphi_{c2}^m)(1-\varepsilon)+\varepsilon](\varphi_{c2}^m - 1)/\eta_{c2}\end{array}}{\tau_1 - E_R b[1-\eta_{t2}(1-a/\varphi_{c2}^m)] - (1-E_R)c}\eta_b \tag{12}$$

where $a = \frac{\eta_{c1}\eta_{t1}\tau_1}{D_0{}^m(\psi_{c1}+1)(\eta_{c1}\eta_{t1}\tau_1 - \psi_{c1})}$, $b = \tau_1(1-\eta_{t1}\psi_{t1})$ and $c = 1+\psi_{c1}/\eta_{c1}$.

To optimize the exergy efficiency, one can derive the following expression from the extremal condition of $\partial\eta_E / \partial\varphi_{c2} = 0$.

The optimal pressure ratio of the compressor 2 corresponding to the optimal exergy efficiency is:

$$\varphi_{c2opt} = \frac{\begin{array}{c}\{abE_R\eta_{t2}[c\varepsilon E_R + b(\varepsilon-1)(E_R-1)(\eta_{t2}-1) - cE_R - \varepsilon] \pm \\ \{ab\eta_{t2}[b(\varepsilon-1)(E_R-1)(\eta_{t2}-1)+\varepsilon(cE_R-1)-cE_R]\times \\ \{c\{-\{bE_R\{\varepsilon(a\eta_{t2}-\eta_{t2}+1)(1-2E_R)+E_R[(2a-2)\eta_{t2}+ \\ \eta_{c2}(\eta_{t2}-2)+2] - \eta_{t2}(a+\eta_{c2}-1)+2\eta_{c2}-1\} - \varepsilon[E_R{}^2\times \\ (\tau_1+1) - E_R(4\tau_1+1)+2\tau_1] + \tau_1[E_R{}^2+2E_R(\eta_{c2}-2)- \\ 2\eta_{c2}+2]\}\} - bE_R\{\varepsilon[(a-1)\eta_{t2}+1](E_R\tau_1-\tau_1+\varepsilon_R)+\tau_1\times \\ \{E_R[\eta_{t2}(1-a)-1]+a\eta_{t2}+(\eta_{t2}-2)\eta_{c2}-\eta_{t2}+1\}\}+ \\ b^2E_R{}^2\eta_{c2}(\eta_{t2}-1) - c^2(E_R-1)[\varepsilon(2E_R-1)+E_R(\eta_{c2}-2)- \\ \eta_{c2}+1] - \tau_1[\tau_1(E_R+\eta_{c2}-1)-\varepsilon(E_R\tau_1+E_R-\tau_1)]\}\}^{1/2}\}^{1/m}\end{array}}{\begin{array}{c}\{[\varepsilon(cE_R-1)+b(\varepsilon-1)(E_R-1)(\eta_{t2}-1)]\times \\ [c(E_R-1)+bE_R(\eta_{t2}-1)+\tau_1]\}^{1/m}\end{array}} \tag{13}$$

And the optimal exergy efficiency is:

$$\eta_{Eopt} = \frac{\begin{array}{c}\eta_{t2}(1-a/\varphi_{c2opt}^m)b - [E_R c(1-\varepsilon) - b\eta_{t2}(1-E_R) \\ \times(1-\eta_{t2}+\eta_{t2}\, a/\varphi_{c2opt}^m)(1-\varepsilon)+\varepsilon](\varphi_{c2opt}^m - 1)/\eta_{c2}\end{array}}{\tau_1 - E_R b[1-\eta_{t2}(1-a/\varphi_{c2opt}^m)] - (1-E_R)c}\eta_b \tag{14}$$

The minimum dimensionless total exergy loss is:

$$\begin{aligned} (e_{loss}/(c_P T_1))_{\min} = \{\tau_1 - E_R b[1-\eta_{t2}(1-\frac{a}{\varphi_{c2opt}^m})] - (1-E_R)c\}/\eta_b - \\ \{\eta_{t2}b(1-\frac{a}{\varphi_{c2opt}^m}) + [E_R c(1-\varepsilon) - b\eta_{t2}(1-E_R)(1-\eta_{t2}+ \\ \eta_{t2}\frac{a}{\varphi_{c2opt}^m})(1-\varepsilon)+\varepsilon](\varphi_{c2opt}^m - 1)/\eta_{c2}\} \end{aligned} \tag{15}$$

4. Numerical examples

In the calculations, it is set that $\eta_{c1} = \eta_{c2} = 0.9$, $\eta_{t1} = \eta_{t2} = 0.85$, $T_1 = 288.15K$, $P_1 = 0.1013MPa$, $P_9 = 0.104MPa$, $D_i = 0.98$ ($i = 1,2,3,4$), $\varepsilon = 0.9$ and $E_R = 0.9$. To see the effects of various parameters on exergy efficiency and other performances of the combined cycle, the results are presented graphically.

Figure 3 shows the influences of the effectiveness (E_R) of the regenerator on the $(\eta_E)_{opt} - \varphi_{c1}$ and $(e_{loss}/(C_P T_1))_{\min} - \varphi_{c1}$ characteristics, respectively. In the range of less than the critical pressure ratio of compressor 1, the optimal exergy efficiency $(\eta_E)_{opt}$ increases with the increase in E_R and the minimum exergy loss $(e_{loss}/(C_P T_1))_{\min}$ decreases with increase in E_R. It reveals that the regenerator can improve exergy performance of the combined cycle.

Figures 4-7 show the influences of the temperature ratio (τ_1) of the Brayton cycle, the effectiveness (ε) of the heat exchanger, the pressure-recovery coefficient (D_i) of each process, the compressor efficiencies (η_{c1} and η_{c2}), as well as the turbine efficiencies (η_{t1} and η_{t2}) on the $(\eta_E)_{opt} - \varphi_{c1}$ and $(e_{loss}/(C_P T_1))_{\min} - \varphi_{c1}$ characteristics, respectively. They show that the optimal exergy efficiency $(\eta_E)_{opt}$ increases with the increases in τ_1, ε, D_i, η_{c1}, η_{c2}, η_{t1} and η_{t2}. The minimum exergy loss $(e_{loss}/(C_P T_1))_{\min}$ decreases with increases in τ_1, ε, D_i, η_{c1}, η_{c2}, η_{t1} and η_{t2}.

Figures 8-12 show the influences of the effectiveness (E_R) of the regenerator, the temperature ratio (τ_1) of the Brayton cycle, the effectiveness (ε) of the heat exchanger, the pressure-recovery coefficient (D_i) of each process, the compressor efficiencies (η_{c1} and η_{c2}), as well as the turbine efficiencies (η_{t1} and η_{t2}) on the $\varphi_{c2opt} - \varphi_{c1}$ characteristics, respectively. They show that the optimal pressure ratio (φ_{c2opt}) of the compressor 2 increases with the increases in τ_1, ε, η_{c2}, η_{t2}, and decreases in E_R, D_i, η_{c1}, and η_{t1}. They also show that the optimal pressure ratio of compressor 2 will equal to 1 when E_R, D_i, η_{c1} and η_{t1} are big enough or η_{c2}, η_{t2} and ε are small enough. In other words, the compressor 2 should be canceled in these extreme conditions.

Figures 13-21 show the influences of the pressure ratio (φ_{c1}) of the compressor 1, the effectiveness (E_R) of the regenerator, the temperature ratio (τ_1) of the Brayton cycle, the effectiveness (ε) of the heat exchanger, the pressure-recovery coefficient (D_i), the compressor efficiencies (η_{c1} and η_{c2}), as well as the turbine efficiencies (η_{t1} and η_{t2}) on the component irreversibilities for the combined cycle, respectively. They show that the exergy loss of the combustion is the largest, and followed by the exergy loss of the heat exchanger.

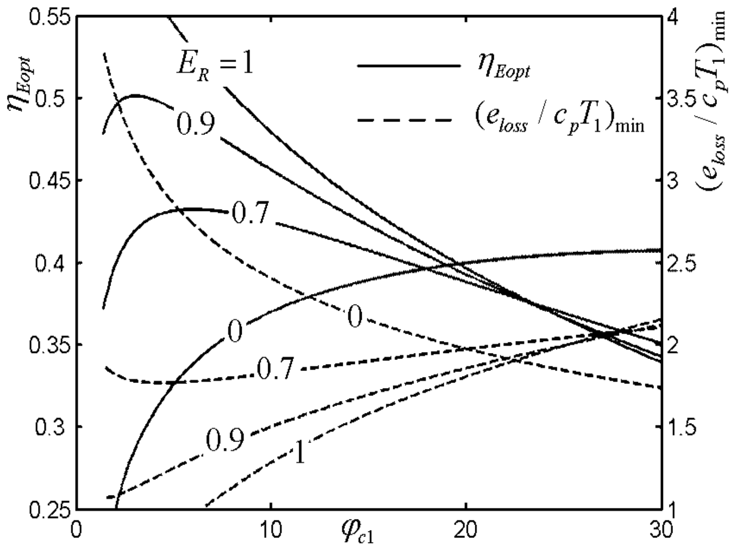

Figure 3. The influence of E_R on the $\eta_{Eopt} - \varphi_{c1}$ and $(e_{loss}/(C_P T_1))_{\min} - \varphi_{c1}$ characteristics

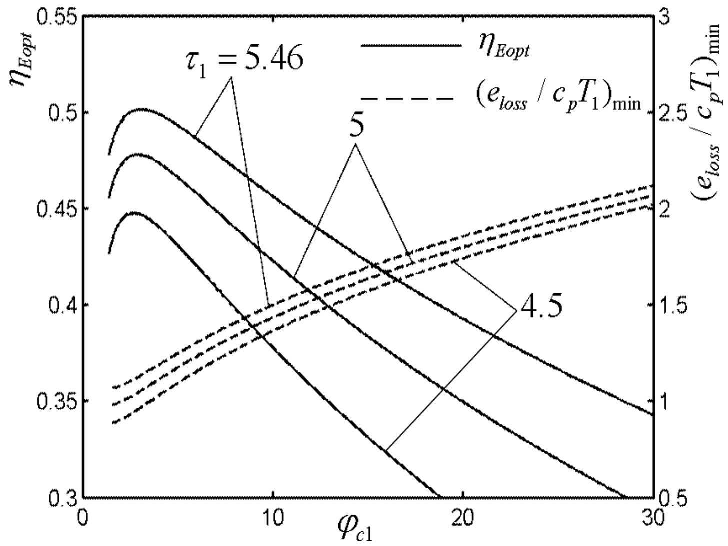

Figure 4. The influence of τ_1 on the $\eta_{Eopt} - \varphi_{c1}$ and $(e_{loss}/(C_PT_1))_{min} - \varphi_{c1}$ characteristics

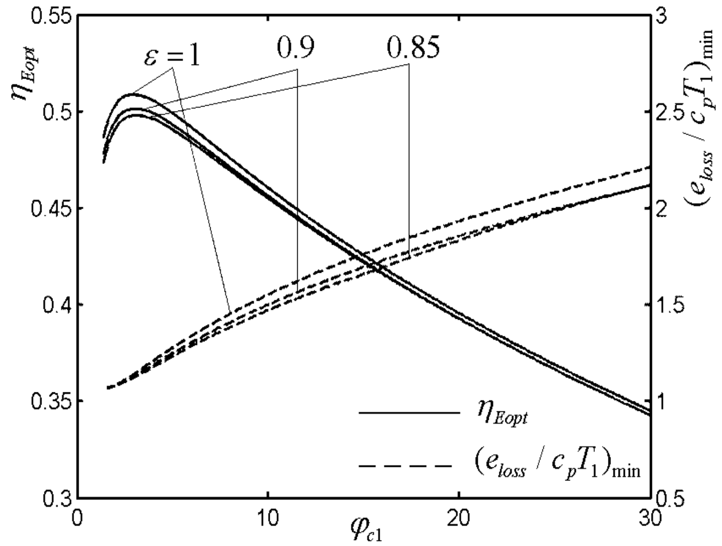

Figure 5. The influence of ε on the $\eta_{Eopt} - \varphi_{c1}$ and $(e_{loss}/(C_PT_1))_{min} - \varphi_{c1}$ characteristics

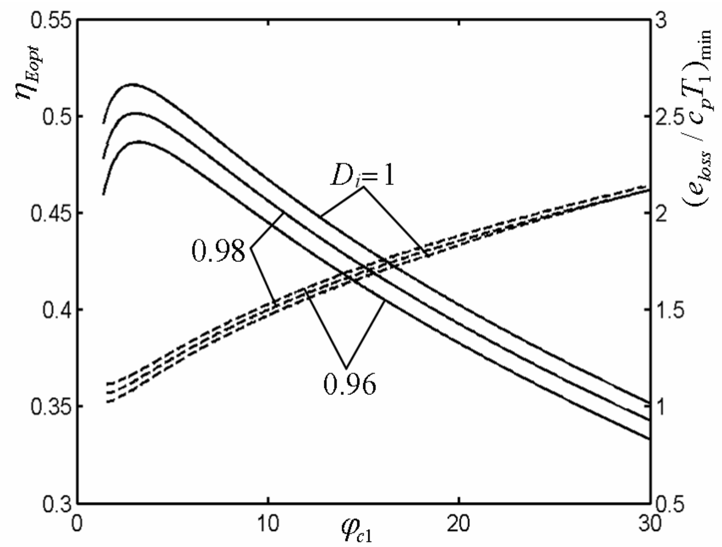

Figure 6. The influence of D_i on the $\eta_{Eopt} - \varphi_{c1}$ and $(e_{loss}/(C_PT_1))_{min} - \varphi_{c1}$ characteristics

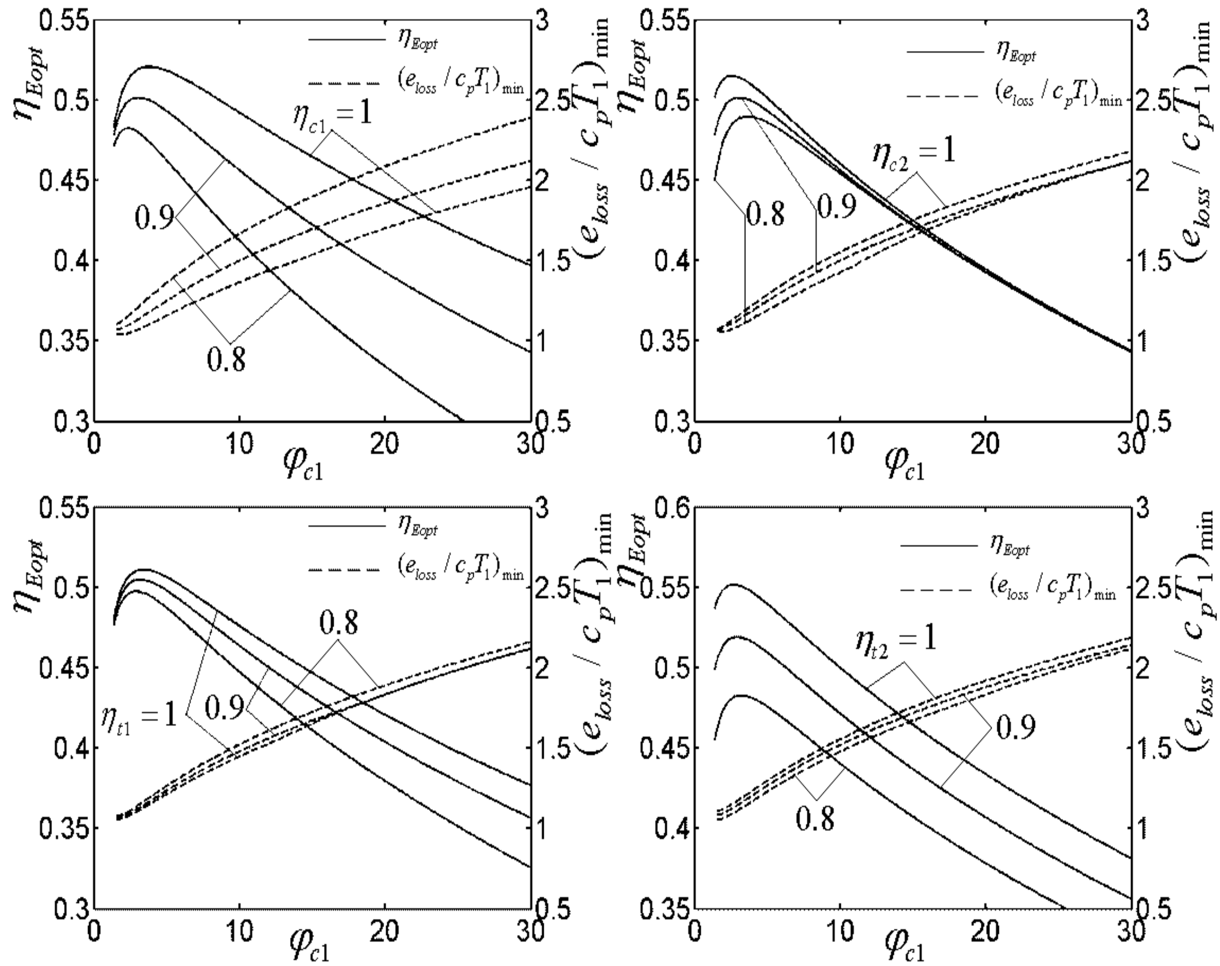

Figure 7. The influence of η_{c1}, η_{c2}, η_{t1} and η_{t2} on the $\eta_{Eopt} - \varphi_{c1}$ and $(e_{loss}/(C_P T_1))_{\min} - \varphi_{c1}$ characteristics

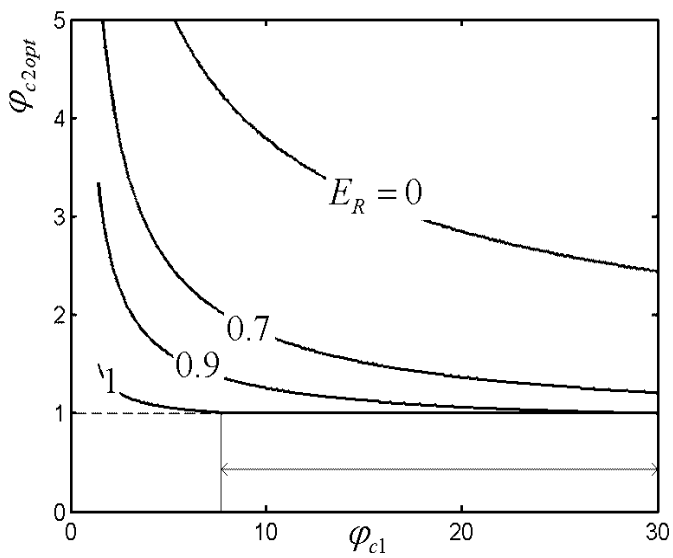

Figures 8. The influence of E_R on the $\varphi_{c2opt} - \varphi_{c1}$ characteristic

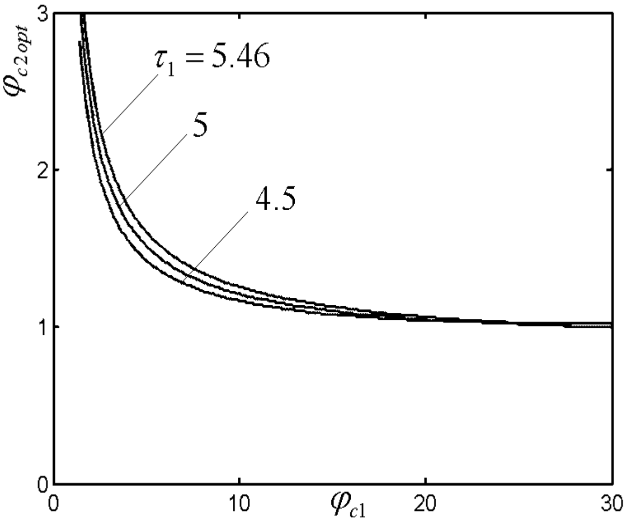

Figure 9. The influence of τ_1 on the $\varphi_{c2opt} - \varphi_{c1}$ characteristic

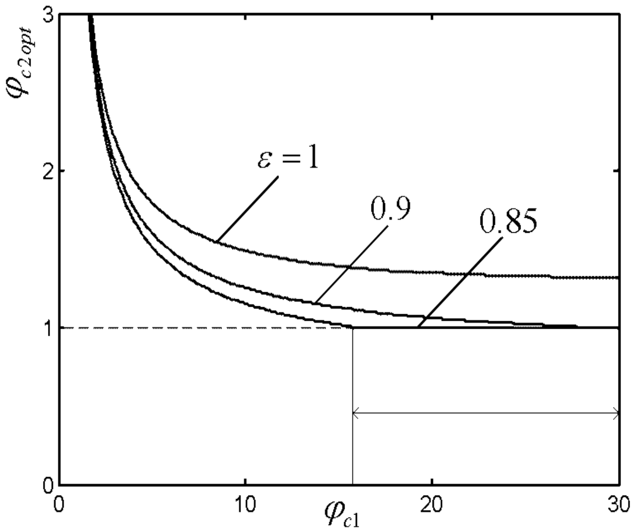

Figure 10. The influence of ε on the $\varphi_{c2opt} - \varphi_{c1}$ characteristic

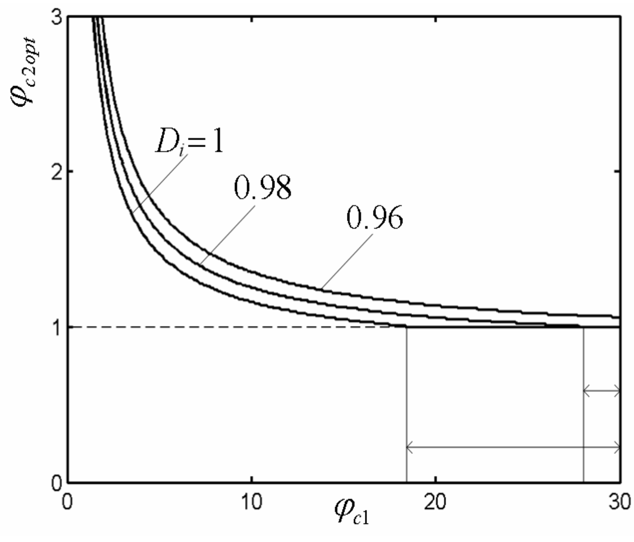

Figure 11. The influence of D_i on the $\varphi_{c2opt} - \varphi_{c1}$ characteristic

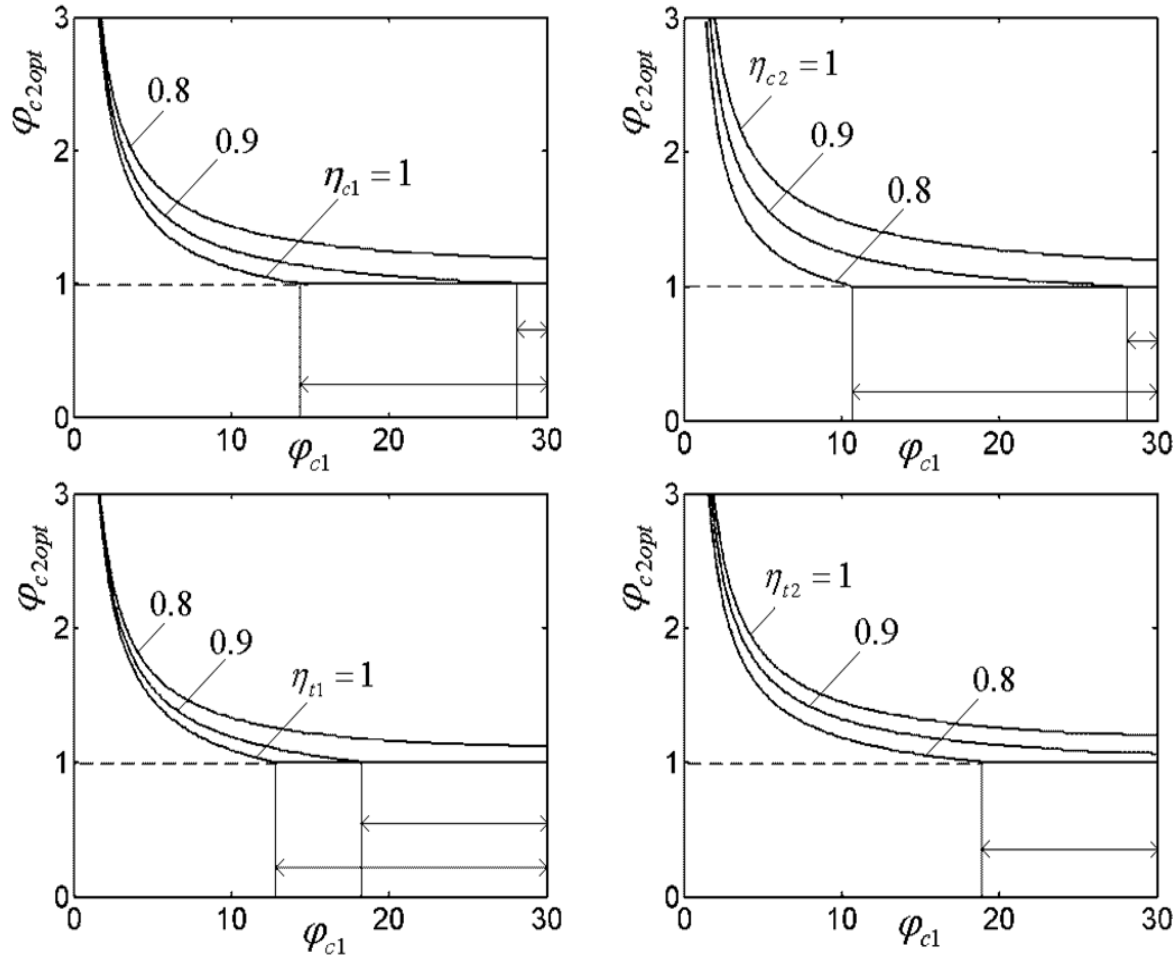

Figure 12. The influences of η_{c1}, η_{c2}, η_{t1} and η_{t2} on the $\varphi_{c2opt} - \varphi_{c1}$ characteristic

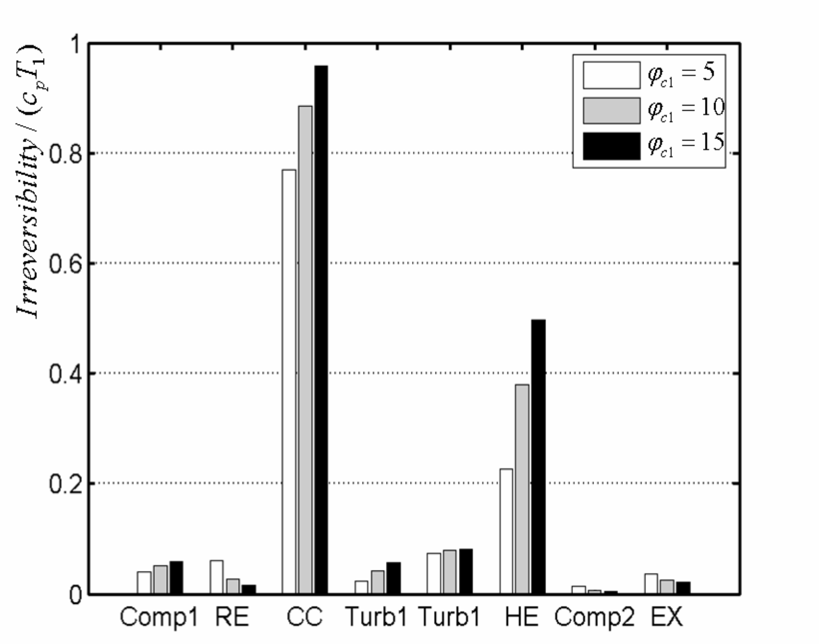

Figure 13. The influence of φ_{c1} on the component irreversibility for the combined cycle

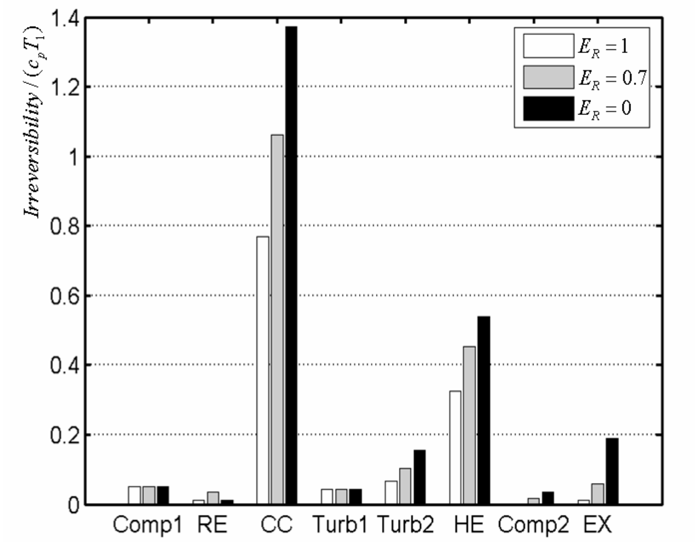

Figure 14. The influence of E_R on the component irreversibility for the combined cycle

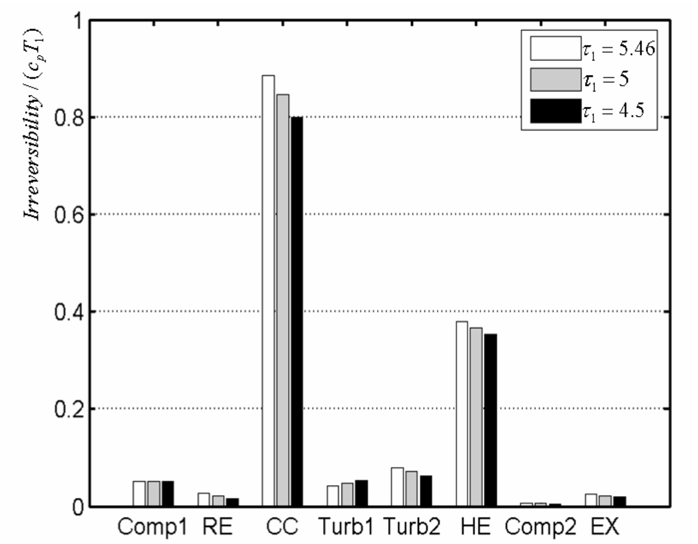

Figure 15. The influence of τ_1 on the component irreversibility for the combined cycle

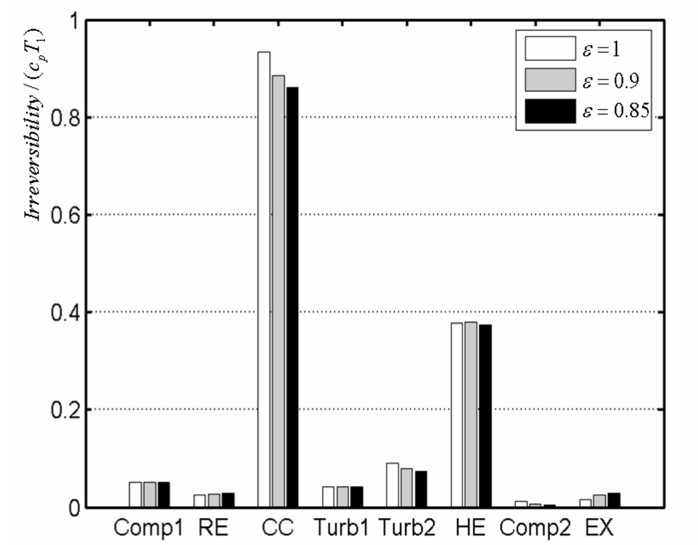

Figure 16. The influence of ε on the component irreversibility for the combined cycle

ISSN 2076-2895 (Print), ISSN 2076-2909 (Online)

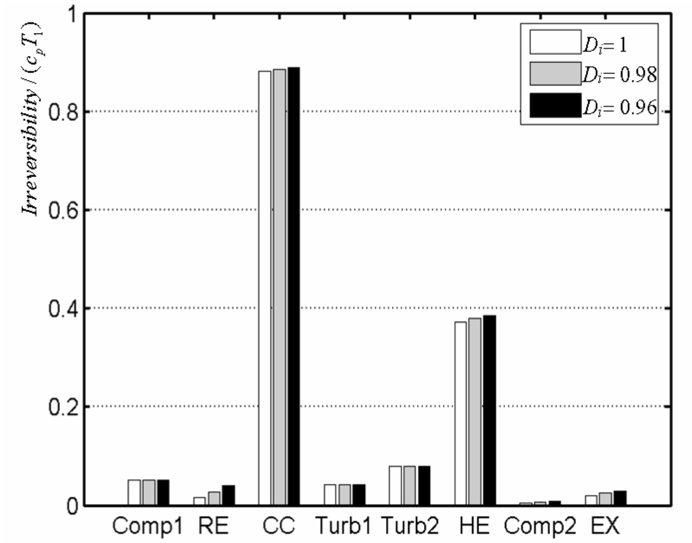

Figure 17. The influence of D_i on the component irreversibility for the combined cycle

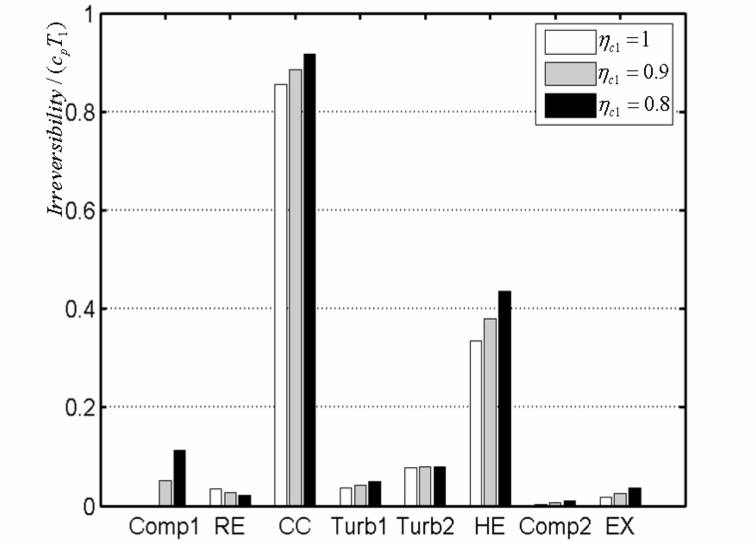

Figure 18. The influence of η_{c1} on the component irreversibility for the combined cycle

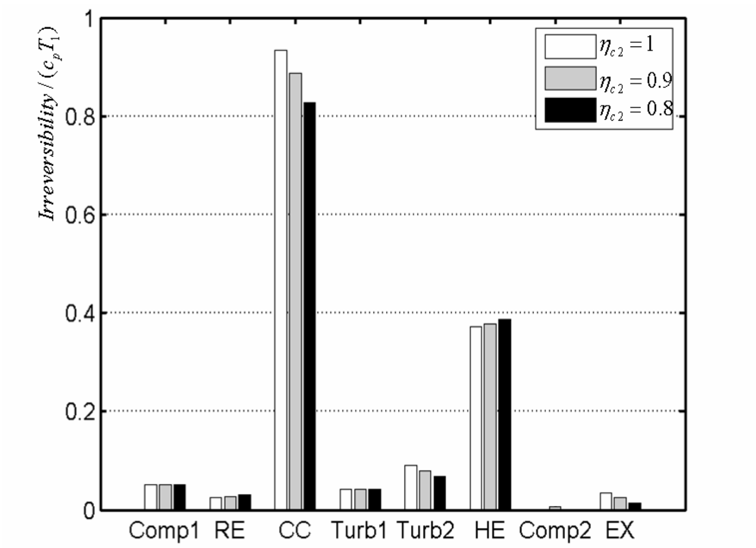

Figure 19. The influence of η_{c2} on the component irreversibility for the combined cycle

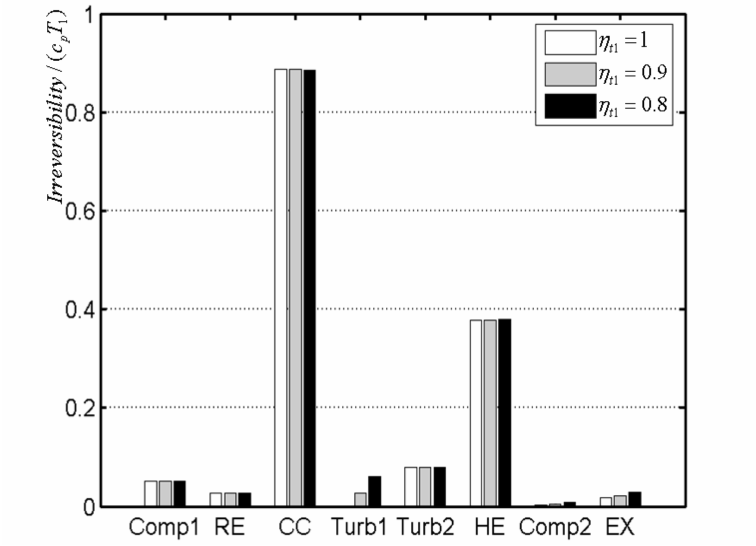

Figure 20. The influence of η_{t1} on the component irreversibility for the combined cycle

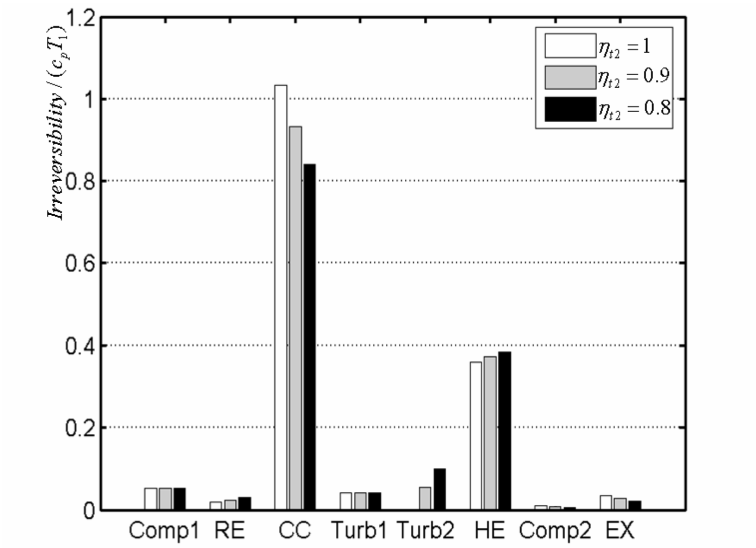

Figure 21. The influence of η_{t2} on the component irreversibility for the combined cycle

5. Conclusion

Exergy analysis and optimization of the combined regenerative Brayton and inverse Brayton cycles with regenerator after the inverse cycle proposed in Ref. [24] has been performed in this paper. The effects of the effectiveness of the regenerator and other parameters on the exergy performances of the combined cycle are analyzed, and the exergy performances are optimized by adjusting the compressor pressure ratio of the bottom cycle. One can see that the base cycle (combined Brayton and inverse Brayton cycle proposed in Ref. [20]) with regenerator can obtain better exergy performance than that of the base cycle. It presents facilitates the design and optimization of complex cycles by pinpointing the exergy losses. The exergy loss of combustion chamber is the largest in the combined cycle and followed by heat exchanger.

Acknowledgments

This paper is supported by The National Natural Science Foundation of P. R. China (Project No. 10905093).

Nomenclature

c	specific heat (kJ/(kgK))
CC	the combustion chamber
$Comp\,1$	the compressor of the regenerative Brayton cycle
$Comp\,2$	the compressor of the inverse Brayton cycle
e	exergy/exergy loss (kJ/kg)
E	the effectiveness of the regenerator/exergy
EX	the exhaust gas of the inverse Brayton cycle
h	enthalpy (kJ/kg)
HE	the heat exchanger of the inverse Brayton cycle
$Irreversibility$	the irreversibility of the component of the combined cycle
k	ratio of the specific heats
P	pressure(MPa)
q	heat (kJ/kg)
T	temperature (K)
$Turb\,1$	the turbine of the regenerative Brayton cycle
$Turb\,2$	the turbine of the inverse Brayton cycle
w	specific work output (kJ/kg)

Greek symbols

ε	the effectiveness of the heat exchanger
φ	pressure ratio
η	efficiency
τ	temperature ratio

Subscripts

b	burning
c	compressor
D	loss
E	exergy
ex	exhaust
f	fuel
g	generator
HE	heat exchanger
in	input
$loss$	total exergy loss
min	mechanical
opt	optimal
out	output
p	pressure
r	rejected
R	regenerator
Q	heat
t	turbine
V	volume
W	work
0	ambient
$1-10$	state points/sequence number

References

[1] Kar A K. Exergy efficiency and optimum operation of solar collectors. Appl. Energy, 1985, 21(4): 301-314.

[2] Nikolaids C, Probert S D. Exergy method for analyzing and optimizing refrigeration processes. Appl. Energy, 1992, 43(4): 201-220.

[3] Bejan A, Tsatsaronis G, Moran M. Thermal Design & Optimization. New York: Wiley, 1996.

[4] Rosen M A. Second law analysis: approaches and implications. Int. J. Energy Res., 1999, 23(5): 415-430.

[5] Bejan A. Fundamentals of exergy analysis, entropy generation minimization, and the generation of flow architecture. Int. J. Energy Res., 2002, 26(7): 545-65.

[6] Rosen M A, Dincer I. Exergy methods for assessing and comparing thermal energy storage systems. Int. J. Energy Res., 2003, 27(4): 415-430.

[7] Kuzgunkaya E H and Hepbasli A. Exergetic performance assessment of a ground-source heat pump drying system. Int. J. Energy Res., 2007, 31(8): 760-777.

[8] Kuzgunkaya E H and Hepbasli A. Exergetic evaluation of drying of laurel leaves in a vertical ground-source heat pump drying cabinet. Int. J. Energy Res., 2007, 31(3): 245-258.

[9] Dincer I, Rosen M A. Exergy. Oxford: Elsevier, 2007.

[10] Ferdelji N, Galovic A, Guzovic Z. Exergy analysis of a co-generation plant. Therm. Sci., 2008, 12(4):75-88.

[11] Hao X, Zhang G. Exergy optimisation of a Brayton cycle-based cogeneration plant. Int. J. Exergy, 2009, 6(1): 34-48.

[12] Bi Y, Wang X, Liu Y, Zhang H, Chen L. Comprehensive exergy analysis of a ground source heat pump system for both building heating and cooling. Appl. Energy, 2009, 86(12): 2560-2565.

[13] Baita M T, Dincer I, Hepbasli A. Energy and exergy analyses of a new four-step copper-chlorine cycle for geothermal-based hydrogen production. Int. J. Hydrogen Energy, 2010, 35(8): 3263-3272.

[14] Kalinci Y, Hepbasli A, Dincer I. Exergetic performance assessment of gasification and pyrolysis processes of pre-treated wood board wastes. Int. J. Exergy, 2011, 8(1): 99-112.
[15] Chase D L. Combined Cycle Development Evolution and Future. GE Power Systems, GER-4206, 2001.
[16] Frost T H, Anderson A, Agnew B. A hybrid gas turbine cycle (Brayton/Ericsson): an alternative to conventional combined gas and steam turbine power plant. Proc. Instn. Mech. Engrs., Part A, J. Power and Energy, 1997, 211 (A2): 121–131.
[17] Zheng J, Sun F, Chen L et al. Exergy analysis for a Braysson cycle. Exergy An Int. J., 2001, 1(1): 41-45.
[18] Fujii S, Kaneko K, Tsujikawa K. Mirror gas turbine: A newly proposed method of exhaust heat recovery. Trans. ASME J. Eng. Gas Turbine and Power, 2001, 123(2): 481-486.
[19] Bianchi M, Negri di Montenegro G, Peretto A. Inverted Brayton cycle employment for low temperature cogeneration applications. Trans. ASME, J. Engng. Gas Turbine Pow., 2002, 124(2): 561-565.
[20] Agnew B, Anderson A, Potts I, Frost TH, Alabdoadaim MA. Simulation of combined Brayton and inverse Brayton cycles. Appl. Therm. Engng., 2003, 23(8): 953-963.
[21] Zhang W, Chen L, Sun F et al. Second-law analysis and optimization for combined Brayton and inverse Brayton cycles. Int. J. Ambient Energy, 2007, 28(1): 15-26.
[22] Alabdoadaim M A, Agnew B, Potts I. Performance analysis of combined Brayton and inverse Brayton cycles and developed configurations. Appl. Therm. Engng., 2006, 26(14-15): 1448-1454.
[23] Zhang Z, Chen L, Sun F. Exergy analysis for combined regenerative Brayton and inverse Brayton cycles. Int. J. Energy and Environment, 2012, 3(5): 715-730.
[24] Zhang Z, Chen L, Sun F. Performance optimization for two classes of combined regenerative Brayton and inverse Brayton cycles. Int. J. Sustainable Energy, 2014, 33(4): 723-741.

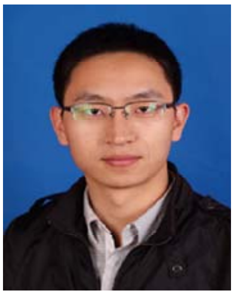

Zelong Zhang received his BS Degree in 2009 from the Huazhong University of Science and Technology and his MS Degree in 2011 from the Naval University of Engineering, P R China. He is pursuing for his PhD Degree in power engineering and engineering thermophysics from Naval University of Engineering, P R China. His work covers topics in finite time thermodynamics and technology support for propulsion plants. Dr Zhang is the author or coauthor of 12 peer-refereed articles (5 in English journals).

Lingen Chen received all his degrees (BS, 1983; MS, 1986, PhD, 1998) in power engineering and engineering thermophysics from the Naval University of Engineering, P R China. His work covers a diversity of topics in engineering thermodynamics, constructal theory, turbomachinery, reliability engineering, and technology support for propulsion plants. He had been the Director of the Department of Nuclear Energy Science and Engineering, the Superintendent of the Postgraduate School, and the President of the College of Naval Architecture and Power. Now, he is the Direct, Institute of Thermal Science and Power Engineering, the Director, Military Key Laboratory for Naval Ship Power Engineering, and the President of the College of Power Engineering, Naval University of Engineering, P R China. Professor Chen is the author or co-author of over 1400 peer-refereed articles (over 620 in English journals) and nine books (two in English).
E-mail address: lgchenna@yahoo.com; lingenchen@hotmail.com, Fax: 0086-27-83638709 Tel: 0086-27-83615046

Yanlin Ge received all his degrees (BS, 2002; MS, 2005, PhD, 2011) in power engineering and enginee thermophysics from the Naval University of Engineering, P R China. His work covers topics in finite thermodynamics and technology support for propulsion plants. Dr Ge is the author or coauthor of ove peer-refereed articles (over 40 in English journals).

Fengrui Sun received his BS Degrees in 1958 in Power Engineering from the Harbing Universit Technology, P R China. His work covers a diversity of topics in engineering thermodynamics, constr theory, reliability engineering, and marine nuclear reactor engineering. He is a Professor in the Colleg Power Engineering, Naval University of Engineering, P R China. Professor Sun is the author or co-auth over 850 peer-refereed papers (over 440 in English) and two books (one in English)